Article

Not peer-reviewed version

Long Distance Movement of *Solanum tuberosum* Translationally Controlled Tumor Protein (*StTCTP*) mRNA

Brenda Xoconostle-Morán , Beatriz Xoconostle-Cázares , Brenda Yazmín Vargas-Hernández , Leandro Alberto Núñez-Muñoz , Berenice Calderón-Pérez , Roberto Ruiz-Medrano *

Posted Date: 19 June 2023

doi: 10.20944/preprints202306.1347.v1

Keywords: TCTP; transient expression; vascular expression; Solanum tuberosum

Article

Long Distance Movement of *Solanum tuberosum* Translationally Controlled Tumor Protein (*StTCTP*) mRNA

Brenda Xoconostle-Morán, Beatriz Xoconostle-Cázares, Brenda Yazmín Vargas-Hernández, Leandro Núñez-Muñoz, Berenice Calderón-Pérez and Roberto Ruiz-Medrano*

Departamento de Biotecnología y Bioingeniería, CINVESTAV-IPN; Avenida Instituto Politécnico Nacional 2508, Col. San Pedro Zacatenco, Ciudad de México 07360, México.

* Correspondence: rmedrano@cinvestav.mx; Tel.: (52-5557473318)

Abstract: The Translationally Controlled Tumor Protein (TCTP) is a multifunctional protein found in most eukaryotic taxa**.** In plants, TCTP regulates cell-cycle progression as well as programmed cell death and is involved in plant regeneration and responses to abiotic and biotic stress, among other functions. Additionally, there is evidence that the transcript and protein are transported over long-distance. Potatoes are a crop of agricultural interest that can reproduce asexually by regeneration from stolons and tubers. Therefore, in this study the effect of transient expression of *Solanum tuberosum* TCTP (*StTCTP*) on tuberization was analyzed. *StTCTP* mRNA was shown to be transported long-distance. Additionally, transient overexpression of *StTCTP* resulted in tuber bearing shoots with a greater diameter compared to control plants. Furthermore, the early stages of tuberization were induced compared to control plants, in which only mature tubers were observed.

Keywords: TCTP; transient expression; vascular expression; *Solanum tuberosum*

1. Introduction

The Translationally Controlled Tumor Protein (TCTP or TPT1), also known as p21 and p23, is ubiquitous in eukaryotic organisms [1]. This protein is involved in a wide range of biological processes and interactions with several biomolecules. Some of these functions include cooperation with anti-apoptotic proteins and mechanisms that promote cell protection [2–5], cellular stress responses [6], regulation of cell cycle and development [7], protein synthesis and degradation, and immune response in animals [8].

There is evidence supporting the anti-apoptotic activity of TCTP, which is influenced by the specific type of cellular stress [8,9]. TCTP contains a BH3-like domain that activates the anti-apoptotic activity of B-cell lymphoma-extra-large protein (Bcl-xL) and stabilizes the induced myeloid leukemia cell differentiation protein (Mcl-1) [3–6,8–11]. The TCTP α-helical domain can enter into the mitochondrial membrane, preventing the dimerization and activation of the pro-apoptotic protein Bax [12]. TCTP binds to the apoptotic protease activating factor 1 (Apaf-1) via its caspase recruitment domain, inhibiting the activation of caspase 9 [13]. TCTP also interacts with p53, promoting its degradation and, in turn, p53 represses TCTP transcription [14,15]. Furthermore, TCTP may act as a heat shock protein with chaperone-like activity in many species[16], as well as preventing oxidative stress-induced cell death in cancer cells [17]. TCTP binds Ca^{2+} protecting cells from Ca^{2+}-dependent apoptosis and acts as a "buffer protein" controlling cellular homeostasis [18]. Moreover, TCTP associates with microtubules in a cell cycle-dependent manner, inducing their rearrangement and increasing microtubule mass and stability [19].

TCTP also plays a crucial role in regulating spindle dynamics during meiotic maturation in bovine and mouse oocytes [20,21]. Additionally, knockout studies in mice have demonstrated that TCTP absence leads to a higher rate of apoptosis, causing embryonic lethality [12,22,23]. In Drosophila, TCTP controls cell and organ size as well as cell number by associating with Rheb, a GTP-binding protein, and displaying guanine nucleotide exchange activity *in vivo* and *in vitro*

Preprints (www.preprints.org) | NOT PEER-REVIEWED | Posted: 19 June 2023 doi:10.20944/preprints202306.1347.v1

[24,25]. Remarkably, Arabidopsis TCTP1 exhibits similar functionality, and Drosophila TCTP can function in Arabidopsis and vice versa [26]. Human *TCTP* mRNA translation is regulated via the mTORC1 pathway through a cis-regulatory element found in its 5'UTR, the 5' TOP motif [23,27,28].

In plants, TCTP has several functions including cell division, growth, development, stress response, photosynthesis, and hormone signaling. TCTP integrates mitotic growth and cell proliferation during organ development by regulating the G1/S transition during cell cycle progression in Arabidopsis and Drosophila [7,26]. Arabidopsis *TCTP* overexpression enhances drought tolerance by rapid ABA-mediated stomatal closure through interaction with microtubules [29]. In tomato, *TCTP* overexpression increases biomass but affects performance under salt and osmotic stress. These phenotypic alterations were associated with up-regulation of genes mainly related to photosynthesis, fatty acid metabolism and water transport [30]. In Arabidopsis, *TCTP* knockdown results in impaired pollen tube growth and general developmental defects. Accordingly, in *Nicotiana tabacum,* TCTP interacts with the Sec7 domain and NtGNL1, essential for polar growth and endocytosis as part of a regulatory network involved in endosomal trafficking in pollen tube growth [31–33] .

There is a wealth of information regarding the long-distance transport of RNAs like mRNAs, long-noncoding RNAs (lncRNAs) and small RNAs (miRNAs, siRNAs and tRNAs fragments, among others), as well as proteins that regulate flower induction, response to phosphate availability, gene silencing, response to pathogen infection and tuber induction in plants [34–40]. Indeed, tomato grafted onto potato rootstocks induced tuber formation indicating the presence of phloem mobile molecules involved in tuber morphogenesis, albeit less effectively than potato scions [41]. Likewise, the overexpression of the transcription factor POTH1, found in phloem, enhances tuber formation *in vitro* [42–45]. POTH1 interacts with StBEL5 to regulate tuber formation. Furthermore, *StBEL5* RNA transport across a graft union to stolon tips correlates with enhanced tuber production [45,46]. In addition, tuber induction involves shoot to root transport of the potato flowering locus T (FT) homolog in response to photoperiod. Similarly, long-distance transport of miRNA 172 also induces tuberization, likely upstream of StBEL5 [39,40].

Both TCTP protein and mRNA are transported over long-distances in cucurbits, Arabidopsis and *N. tabacum* [47–50]. The presence of TCTP in the proteomes and transcriptomes of phloem exudates from other species suggests that this is a more general phenomenon in vascular plants [51–53]. Long-distance transport of the Arabidopsis TCTP2 (AtTCTP2) protein and mRNA is associated with adventitious roots formation in tobacco, which potentially underlies the ability of this gene to induce whole plant regeneration [48,49,54]. Additionally, we have proposed the existence of two main types of TCTP in plants based on their predicted structure and the ability to induce *in vitro* plant regeneration [55]. AtTCTP2-like proteins as *Cucurbita maxima* TCTP (CmTCTP) share this *in vitro* plant regeneration activity possibly derived from a proposed role in asexual reproduction, while AtTCTP1-like proteins lack this property [49].

The potato genome harbors a single *TCTP* gene (*StTCTP).* The predicted structure of the encoded protein is similar to AtTCTP2-like proteins, thus may be related to plant regeneration. Therefore, we analyzed whether *StTCTP* mRNA is transported to apical leaves and roots and if this causes a phenotypic modification after agroinfiltration of a *StTCTP*::*GFP* construct in potato. Our results indicated that *StTCTP* mRNA has the capacity to move long-distance, and its transient expression induces changes in tuberization.

2. Results

2.1. GFP-fused StTCTP transcript is transported long distance

Previously, *AtTCTP2* was shown to be a functional gene and to be transported long distance through a graft union in tobacco, in addition to promoting regeneration and increasing biomass in tobacco [49]. Given its predicted structural similarity, we hypothesize that *StTCTP* gene may play a role in regeneration and thus in vegetative reproduction in potato. To explore this possibility, the *StTCTP* open reading frame (ORF) fused to GFP was cloned under the control of the 35S promoter

Preprints (www.preprints.org) | NOT PEER-REVIEWED | Posted: 19 June 2023 doi:10.20944/preprints202306.1347.v1

for agroinfiltration of leaves of 3-week-old potato plants. *Agrobacterium rhizogenes* was used because in previous studies we found that *CmTCTP* and *AtTCTP2* were able to induce whole plant regeneration in tobacco using this strain [47,49]. Subsequently, endpoint RT-PCR was performed to detect the transcript of the reporter gene in agroinfiltrated and apical (systemic) leaves. GFP was detected in the systemic leaves of 24 out of 30 plants agroinfiltrated with the vector harboring the *StTCTP*::*GFP* construct (Figure 1). In contrast, *GFP* mRNA was not detected in the apical leaves of plants agroinfiltrated with the vector harboring the *GFP*::*GUS* construct (Figure S1).

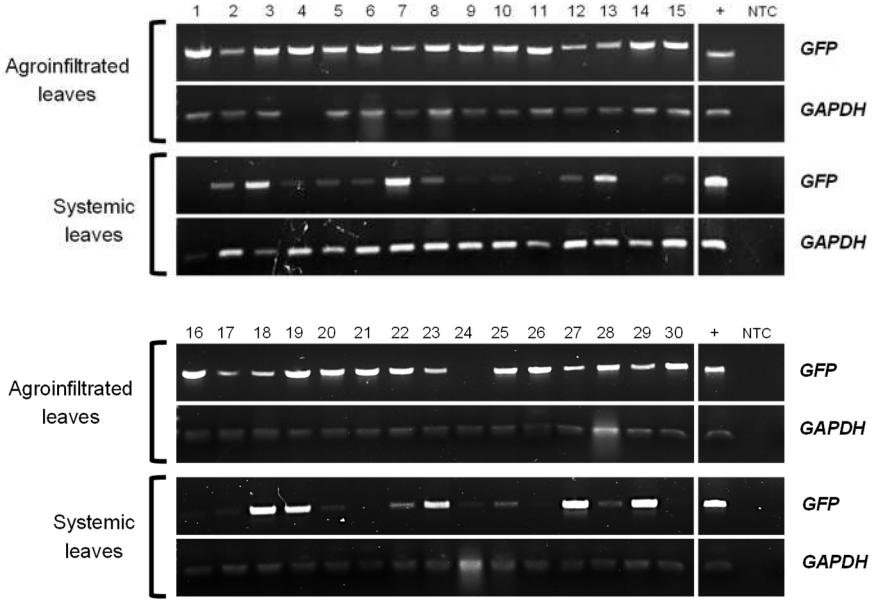

Figure 1. *GFP* and *GAPDH* mRNA detection in agroinfiltrated and systemic leaves from potato plants transiently transformed with *StTCTP::GFP* construct. Agarose gel electrophoresis of endpoint RT-PCR products from total RNA of transiently transformed plants (1-30). *GFP*: green fluorescent protein, reporter gene (720 bp). *GAPDH*: glyceraldehyde-3-phosphate dehydrogenase, endogenous gene (92 bp). +: positive control. NTC: non-template control.

These results were corroborated by RT-qPCR of leaves from nine samples in which the *GFP* transcript was detected in systemic leaves of agroinfiltrated plants with *StTCTP::GFP* construct and compared with *GFP::GUS*-harboring vector plant samples (Figure 2). *StTCTP* transcript was transported from agroinfiltrated to systemic leaves (Figure 2A). Additionally, the *StTCTP*::*GFP* transcript was also found in the roots of agroinfiltrated plants with the *StTCTP*::*GFP* construct (Figure 2A and 2B). In contrast, the *bar* mRNA was detected only in leaves of agroinfiltrated plants with either the control or the *StTCTP*::*GFP* constructs (Figure 2C). Endogenous *StTCTP* mRNA was also detected in the apex, leaf, stem, root, and callus to determine the accumulation sites of this transcript (Figure S2). There was a greater accumulation of *StTCTP* mRNA in the stem and root, later in the apex, leaf, and callus.

Preprints (www.preprints.org) | NOT PEER-REVIEWED | Posted: 19 June 2023 doi:10.20944/preprints202306.1347.v1

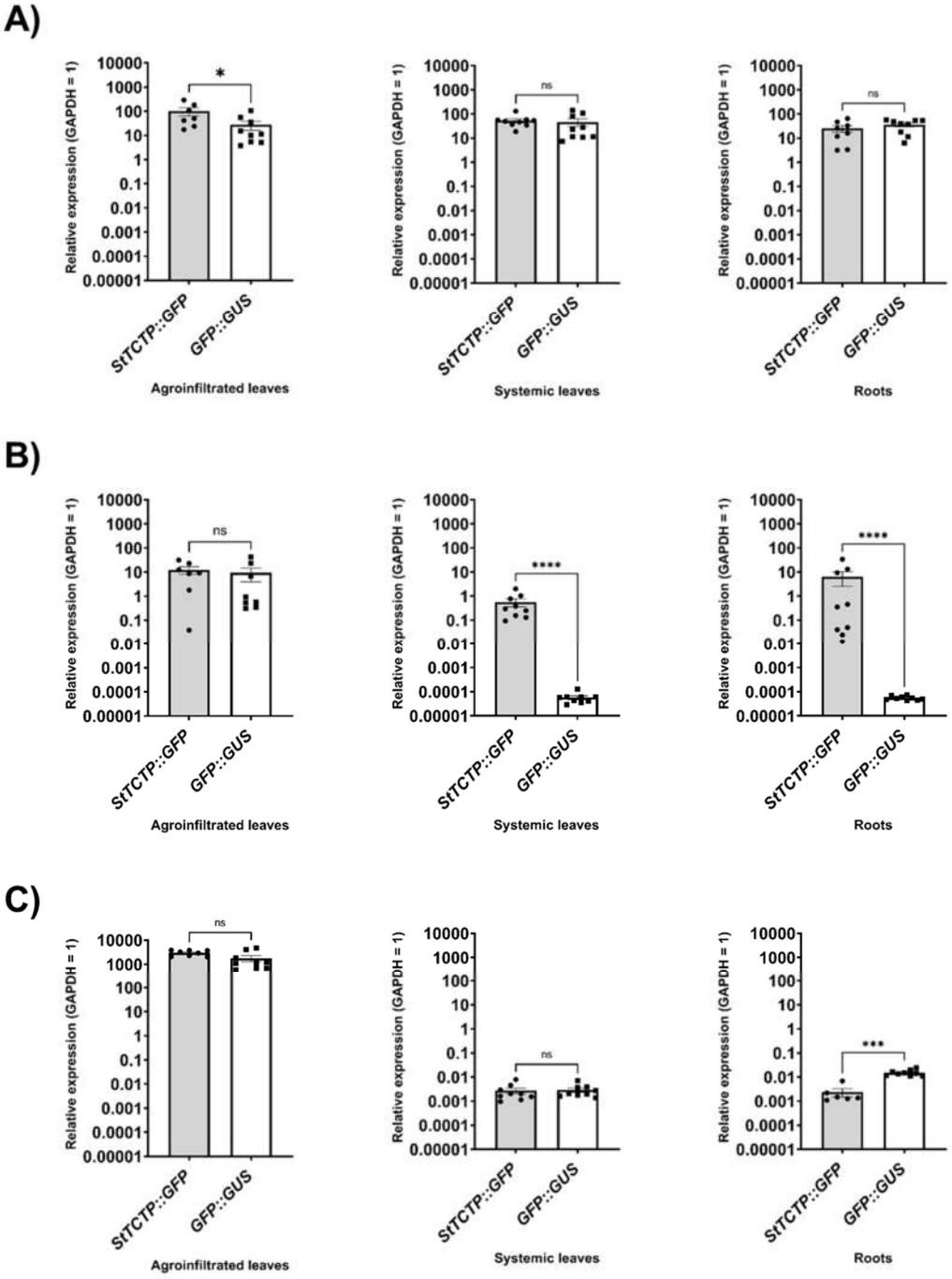

Figure 2. *StTCTP*, *GFP* and *bar* mRNA relative expression in agroinfiltrated, systemic leaves and roots from potato plants transiently transformed with *StTCTP::GFP* or *GFP::GUS*. Transcript levels of A) *TCTP*, B) *GFP* and C) *bar*, in plants agroinfiltrated with *StTCTP*::*GFP* or *GFP*::*GUS* constructs. Data dispersion is represented with black circles and squares, respectively. n = 9 in all cases. Bars represent standard error of the mean. Asterisks symbolize significant difference according to Mann-Whitney tests: *P<0.05, ***P<0.005 and ****P<0.0001; not significant (ns).

2.2. Phenotype of plants agroinfiltrated with StTCTP::GFP or GFP::GUS

The phenotype of the agroinfiltrated plants with *StTCTP::GFP* or *GFP::GUS* were evaluated to determine whether *StTCTP* generates changes in tuberization stage and the leaf area.

Preprints (www.preprints.org) | NOT PEER-REVIEWED | Posted: 19 June 2023 doi:10.20944/preprints202306.1347.v1

2.2.1. StTCTP induces an increase in stolon diameter and early stages of tuberization

To determine whether *StTCTP*::*GFP* has an effect on the phenotype of tubers, agroinfiltrated potato plants were grown and maintained until their formation. Biomass, diameter and number of tubers per plant were measured (Figure S3). No significant differences between plants agroinfiltrated with *StTCTP*::*GFP* and control plants (agroinfiltrated with *GFP*::*GUS*) regarding tubers per plant were found. However, *StTCTP* appeared to increase tuber induction since eight plants treated with *StTCTP*::*GFP* harbored tubers in immature stages of tuberization (stages I–VII [56]) compared to control plants in which only mature tubers (stage VIII) were observed (Figure 3; Table S1).

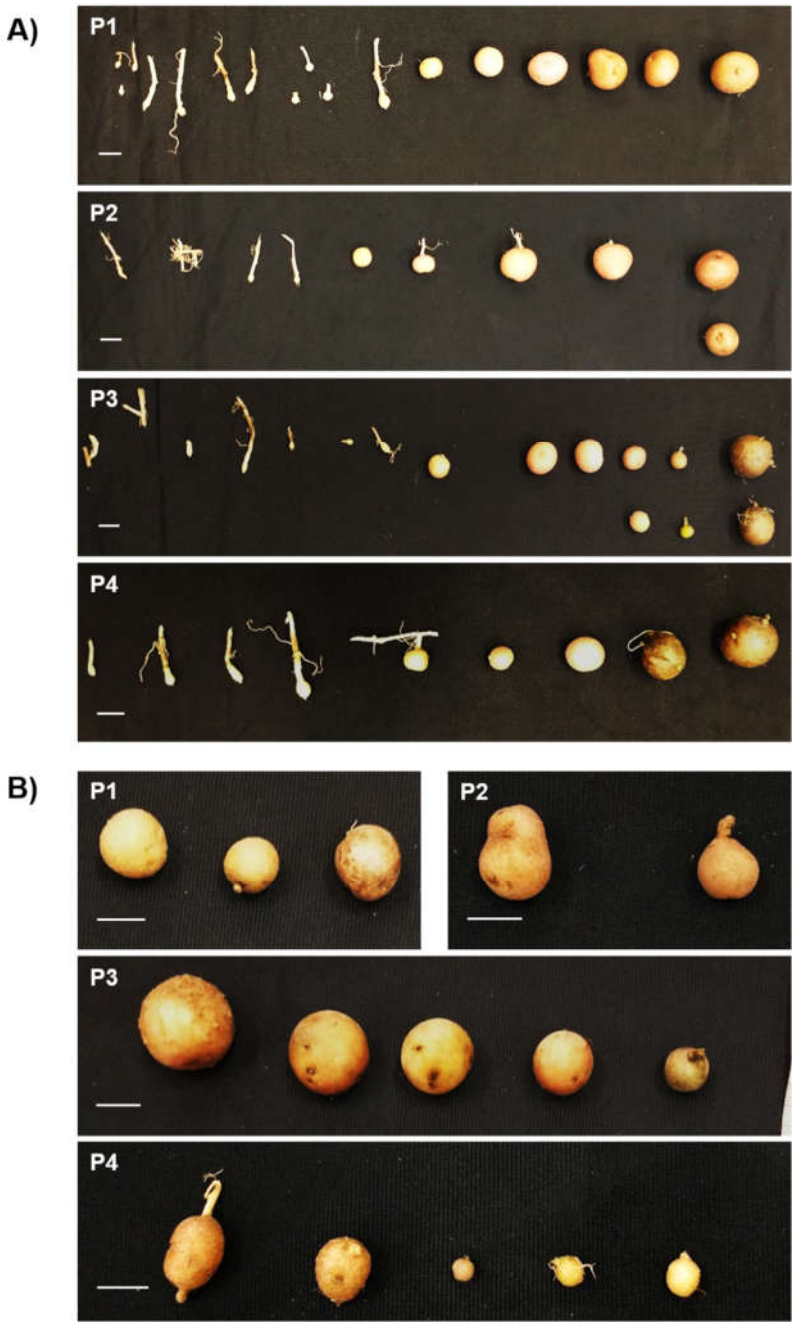

Figure 3. Induction of tuber formation in plants agroinfiltrated with *StTCTP*::*GFP*. Tubers were collected two months after agroinfiltration. A) Stolon stages up to mature tuber from four independent plants (P1-P4) agroinfiltrated with the *StTCTP*::*GFP* construct. B) Tubers that emerged from four plants (P1-P4) agroinfiltrated with *GFP*::*GUS*, all of which were mature tubers; additionally, no stolons were observed. Scale bars = 1 cm.

Preprints (www.preprints.org) | NOT PEER-REVIEWED | Posted: 19 June 2023 doi:10.20944/preprints202306.1347.v1

In addition, formation of seedlings and stolon in three out of thirty plants was observed in plants agroinfiltrated with *StTCTP::GFP* (in which the *GFP* amplicon was detected). In contrast, no seedlings or stolons were observed in plants agroinfiltrated with *GFP::GUS* (0/30; Figure 4).

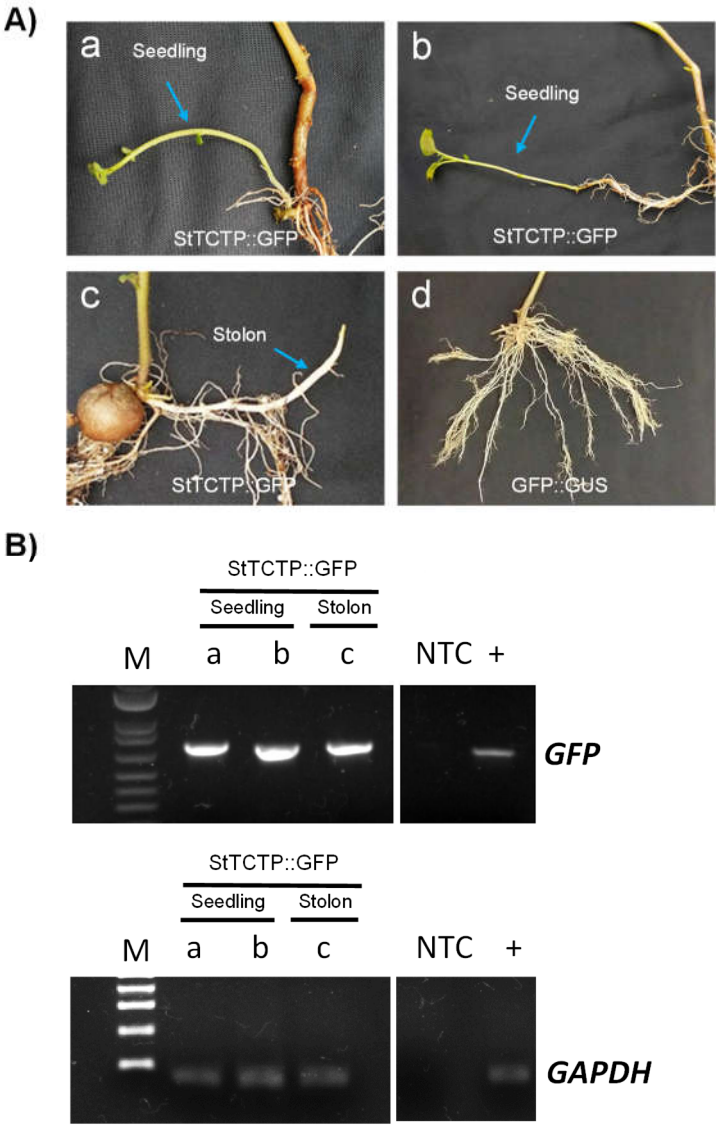

Figure 4. Induction of seedling formation as a result of agroinfiltration with *StTCTP*::*GFP*. A) Emerging seedlings (a and b) and stolon (c) after two weeks post agroinfiltration with *StTCTP*::*GFP*. Plants agroinfiltrated with the *GFP::GUS* did not show seedling nor stolon formation two weeks after treatment (d). B) Detection of *GFP* and *GAPDH* by endpoint RT-PCR of seedlings (a and b) and stolon (c). M: molecular marker, 1 kb Plus DNA ladder (Invitrogen); +: positive control; NTC: non-template control.

2.2.2. StTCTP promotes increase in shoot diameter

In order to analyze the phenotype of mature tubers of plants agroinfiltrated with *StTCTP::GFP*, a shoot generation assay was carried out. First, all the shoots of the *StTCTP::GFP* plants showed purple pigmentation indicating strong anthocyanin accumulation, while those from plants agroinfiltrated with the control vector did not show any pigmentation (Figure 5A and 5B). Second, stolon number per tuber and the sprout length did not show significant difference. However, the shoot diameter was larger in the emerging tubers in *StTCTP::GFP*-treated plants compared to those agroinfiltrated with *GFP::GUS* (Figure 5C to 5E).

Preprints (www.preprints.org) | NOT PEER-REVIEWED | Posted: 19 June 2023 doi:10.20944/preprints202306.1347.v1

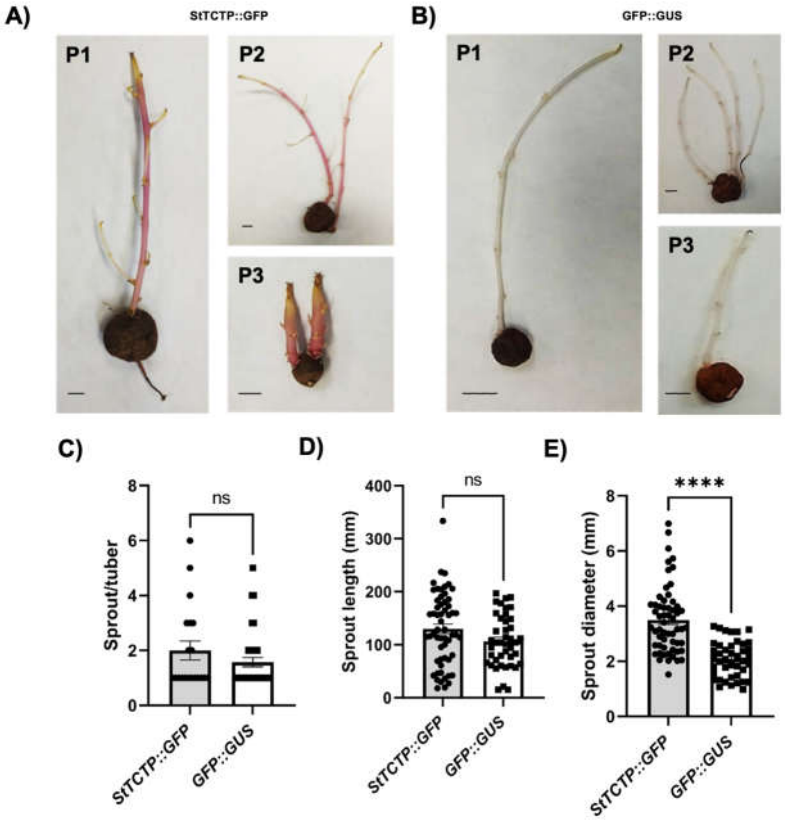

Figure 5. Phenotype of tubers from agroinfiltrated plants. A) Tubers were collected two months after agroinfiltration. These were incubated at 4°C in dark conditions to visualize shoot emergence in plants (P1-P3) agroinfiltrated with *StTCTP::GFP* (A) and *GFP::GUS* (B). Number of stolons per tuber (C) sprout length (D) and diameter (E) were determined in plants agroinfiltrated with either *StTCTP::GFP* or *GFP::GUS* constructs; data dispersion is represented with black circles and squares, respectively. Scale bars = 1 cm. Sprout/tuber (*StTCTP::GFP* n=20; *GFP::GUS* n= 37). Sprout length and diameter (*StTCTP::GFP* n=58; *GFP::GUS* n= 42). Bars represent standard error of the mean. Asterisks indicate significant difference according to Mann Whitney tests: ****P<0.0001; not significant (ns).

2.3. Molecular docking simulation indicates interaction between StTCTP and PTB1/6

Next, prediction of the *StTCTP* transcript 3D structure and docking with PTB1 and PTB6 proteins, reported to bind *StBEL5* RNA [57,58] were carried out. mRNA sequences of *StTCTP*, *AtTCTP1*, *AtTCTP2*, *CmTCTP* and *StBEL5* were obtained as indicated in the methods section. The models with the best scores and criteria were chosen for further analysis (Table S2 and S3). On the other hand, for 3D structure prediction of StPTB1 and StPTB6, the models with best scores and validation values were also selected (Table S4 and S5). Finally, for the protein-RNA docking, the interaction models with the highest confidence scores were analyzed (Table S8). The results suggested that *StTCTP* mRNA could interact with these proteins and may be transported to roots, where it could participate in regulation of tuber formation. Hypothetical interactions of *AtTCTP1*, *AtTCTP2*, *CmTCTP*, *StBEL5* (control) with PTB1 and PTB6 were also predicted (Figure S6).

3. Discussion

The long-distance transport of proteins and RNAs (e.g., miRNAs, mRNAs, siRNAs, and lncRNAs), appears to regulate processes that require communication between distant plant tissues. Examples of these processes include flower and tuber induction, which are mediated by the FT protein and its homologs, tuber induction by miRNA172 and *StBEL5* mRNA, response to phosphate deficiency by miRNA399 and other mRNAs, and silencing by siRNAs, among many others [34,37,39,40]. It has been determined that TCTP protein and mRNA display long-distance movement

 doi:10.20944/preprints202306.1347.v1

and have been found in phloem proteomes and transcriptomes across different species. TCTP has the potential to induce regeneration and adventitious roots across graft junctions. However, it remains unclear whether TCTP functions are linked to its mobility to distant tissues. *CmTCTP* and *AtTCTP2* have been shown to induce plant regeneration, suggesting their potential association with asexual reproduction in plants [59]. Considering the structural similarity between these proteins, it can be hypothesized that StTCTP shares common functions [55].

Transient transformation assays indicated that StTCTP functions in a non-cell autonomous manner. Our results demonstrated the bidirectional transport of *StTCTP* mRNA from agroinfiltrated leaves to apical tissues and roots. In our analysis, the ORF was used, as prior studies have established that *TCTP* mRNA transport does not require 5'- or 3'-UTR. In addition, it has been demonstrated that *AtTCTP1* ORF (spanning from the start codon to position 285) is able to mediate the transcript mobility [48,60]. *GFP* mRNA levels in systemic leaves of plants agroinfiltrated with *StTCTP::GFP* were higher than in the *GFP::GUS*-treated plants, indicating the presence of the recombinant transcript in the apical portions of these plants (which was also observed by endpoint RT-PCR). This finding supports the notion that *StTCTP* mRNA, such as *CmTCTP* and *AtTCTP2,* is transported over long distances.

Agroinfiltrated plants were maintained in greenhouse until mature tuber emergence, to determine the potential effects of *StTCTP* overexpression on their phenotype. In our study, no significant differences were observed in tuber number per plant, mass, or size. However, we observed a trend towards a larger number per plant and diameter of tubers in *StTCTP::GFP*-treated plants compared to the control group, supporting the notion that this gene is involved in the tuberization process. Importantly, *StTCTP*-treated plants harbored tubers at different stages of immature development, in contrast to control plants, in which these were not observed. A similar trend towards an increase in aerial biomass of plants that were agroinfiltrated with *StTCTP::GFP* was also observed, which is consistent with the observation that tomato *TCTP* overexpression in tobacco causes an increase in biomass [30]. The induction of tubers in early stages of development after agroinfiltration with the vector harboring *StTCTP::GFP* suggests that *StTCTP* could play a role in tuber formation. Furthermore, we found leaf-to-root transport of *StTCTP* mRNA, presumably through the phloem, which is supported indirectly by the presence of *TCTP* mRNA and protein in phloem exudates and its expression in phloem in other species. Similarly, *StBEL5* mRNA is phloem mobile, enhancing tuberization by targeting genes that control growth [46]. It is becoming increasingly clear that there are multiple phloem-mobile signals that control tuberization, either its induction or development, although their hierarchy is less clear, since it appears that there are several independent pathways regulating tuber development. Thus, *StTCTP* may be involved more directly in tuber development. It will be of interest to determine the pathway in which it acts in this process.

StTCTP::GFP mRNA levels are 1 to 2 orders of magnitude lower than the endogenous *StTCTP* mRNA (as determined by *GFP* mRNA accumulation) (Figure 2). While this is expected given the transient nature of the transformation method, it is interesting to note that even this modest increase of transcript was able to induce a phenotype in roots, i.e, induction the immature development stages (I-VII) of tuberization. It is of great interest to analyze if both expression and long-distance transport of StTCTP protein and mRNA are tightly regulated. Another effect of *StTCTP* overexpression was the accumulation of anthocyanins, antioxidant compounds that promote tolerance to biotic and abiotic stress [61], possibly related with TCTP function of tolerance to different types of stress in plants. Thus, it can be proposed that overexpression of *StTCTP* could lead to an abnormal phenotype due to the unregulated transport of mRNA. An important effect observed was the formation of seedlings from stolons, which is a common mechanism for asexual plant reproduction, which may bear relation to the ability of *CmTCTP*, *AtTCTP2* and, possibly, *StTCTP* to induce whole plant regeneration. It must be mentioned that plant regeneration mediated by the former two requires *A. rhizogenes* and, more precisely, its *rol* genes. It will be of interest to determine if this phenomenon occurs independently of *A. rhizogenes* in a species that is able to reproduce asexually from stolons such as potato.

Although *StTCTP*, is most actively expressed in stems and roots, and at lower levels in leaves and apical tissue, it is not clear why it is transported to long-distance tissues. It could be interpreted

 doi:10.20944/preprints202306.1347.v1

that some extra input of the gene product from source tissues are required in apices. However, it is of great interest to determine source tissues for long-distance transport of *StTCTP* in wild type plants.

Given that *StBEL5* mRNA interacts with StPTB1/6, which are members of the PTB family of RNA-binding proteins that regulate specific stages of development through an interaction with phloem-mobile transcripts [57,58], the potential interaction of the *StTCTP* transcript with these proteins was analyzed through molecular docking. The results indicated that this transcript could bind to PTB1/6 according to *in silico* predictions, suggesting that *StTCTP* may also be transported and its activity regulated by the StPTB family. Furthermore, our results indicated that the phloem-mobile transcripts *AtTCTP1*, *AtTCTP2*, *CmTCTP* and *StBEL5* are also predicted to bind PTB1/6.

4. Materials and Methods

4.1. Plant material

Potato (*Solanum tuberosum* L. cv. Cambray) tubers were disinfected with 1% Tween-20 and distilled and sterile water, incubated in the dark until sprouts emerged (about 2 weeks), and planted in sterile soil (soil:peat moss:agrolite; 2:2:1) in pots 40 cm long and sheltered in greenhouse. The soil was constantly stirred to allow aeration of emerging roots and tubers.

Callus induction was performed as described previously [62] for determination of endogenous *StTCTP* mRNA levels. Stem explants previously disinfected with 0.5% bleach and abundantly washed with water, were placed in MS medium (1.0 MS salts, 2% sucrose, and 0.4% Gelrite Gelrite agar) supplemented with 0.5 mg/L 2,4-D and 2.0 mg/L BA and incubated in dark conditions until callus formation (10 days). All reagents used were purchased from Sigma-Aldrich (St. Louis MO), unless otherwise stated.

4.2. RNA extraction and vector construction

RNA was extracted from 1 g of ground tissues (leaf, root and callus) using the guanidine hydrochloride method [63]. First strand cDNA was synthesized using Superscript III (Thermo Fisher, Waltham MA) following the manufacturer's recommendations, and the *StTCTP* ORF was amplified using Takara ExTaq (Takara Bio USA, San Jose CA) with *StTCTP*-specific primers (without stop codon; Table S7) the conditions of the endpoint PCR were follows: 30 cycles of denaturation (98°C, 10 s), primer annealing (60°C, 30 s), and primer extension (72°C, 1 min). The amplification product was cloned into the pCR8/GW/TOPO vector (Invitrogen, Thermo Fisher) and its orientation was confirmed by PCR, digestion and sequencing. The entry clone was recombined into the pB7FWG2,0 binary vector through Gateway cloning to obtain the *StTCTP* ORF fused to the *GFP* ORF (*StTCTP::GFP*) under the control of the CaMV 35S promoter. Similarly, the e35S promoter from pBUN4U6SM vector [64] was amplified by PCR which was introduced into the pBGWFS7 binary vector also by Gateway cloning for use as a control (*GFP::GUS* vector). Both the *StTCTP::GFP* and *GFP::GUS* constructs were used to transform *A. rhizogenes* (strain K599) by electroporation, as previously described [46]. Candidate clones were verified by PCR.

4.3. Potato transient transformation

Transient transformation was carried out by agroinfiltration of 3-week-old potato after sprout emerged. Three leaves distal to apical and root meristems were chosen to perform the agroinfiltration procedure [65]. Briefly, *A. rhizogenes* K599 carrying the *StTCTP::GFP* vector was cultured in YEB medium (1 g/L yeast extract, 5 g/L peptone, 5 g/L sucrose, 0.5 g/L $MgCl_2$) supplemented with antibiotics (spectinomycin 100 mg/L) and incubated for 48 h at 28 °C at 150 rpm. Subsequently, the bacterial culture was pelleted by centrifugation at 3000 g for 15 min at 4 °C. The resulting pellet was resuspended in infiltration medium (10 mM $MgCl_2.7H_2O$, 10 mM 2-[N-morpholino] ethanesulfonic acid (MES) pH 5.6 and 200 μM acetosyringone) until reaching an OD600 equal to 0.8. *A. rhizogenes* suspension was injected to the abaxial surface of the leaf. One week post infiltration, tissues were collected for detection by endpoint RT-PCR and RT-qPCR.

Preprints (www.preprints.org) | NOT PEER-REVIEWED | Posted: 19 June 2023 doi:10.20944/preprints202306.1347.v1

4.4. Endpoint RT-PCR

Plant tissues (agroinfiltrated leaves, systemic apical leaves and roots) were collected for RNA extraction as previously described. cDNA synthesis was carried out with WarmStart® RTx Reverse Transcriptase (New England Biolabs; Beverly MA) according to the supplier's recommendations. Briefly, the kit components (final concentrations: 1X Isothermal Amplification Buffer, dNTP Mix (0.5 mM), Random Primer Mix (6 µM), RNase Inhibitor-Murine (20 units), WarmStart RTx Reverse Transcriptase (0.25 µl) were homogenized with target cDNA at a concentration of 100 ng/µL. Mix was incubated for 5 minutes at 25°C for annealing, 10 minutes at 55°C for synthesis and 10 minutes at 80°C for enzyme inactivation. cDNA was used for endpoint PCR to detect the *GFP* and *GAPDH* transcripts (Table S7) using Platinum® Taq DNA Polymerase (Invitrogen, Thermo Fisher) following the manufacturer's recommendations.

4.5. Quantitative RT-PCR (RT-qPCR)

GFP, *StTCTP*, *bar* and *GAPDH* transcript levels were determined by RT-qPCR. 50 ng/µL of RNA was mixed with the KAPA SYBR® FAST qPCR Master Mix reagents following the user manual specifications (Merck; Rahway NJ). Specific primers for *GFP*, *StTCTP*, *bar* [66] and *GAPDH* (Table S7) were used to set up the RT-qPCR reaction. The mix was incubated in Step One Plus Real-Time PCR System under the following conditions: the holding stage consisted in 5 min at 42°C for reverse transcription, the next step was 5 min at 95°C, the cycling stage comprised 95°C per 5 s and 60 °C per 20 s with 40 cycles, the melt curve stage consisted of 15 s at 95°C and 1 min at 60°C, finally, 15 s al 95°C to assure no additional products amplified in the reaction. Each sample was analyzed by triplicate. *GAPDH* was used to normalize transcript accumulation. The $2^{-\Delta\Delta Ct}$ method was used to calculate relative transcript accumulation [67].

4.6. Shoot induction assay

Tubers of plants agroinfiltrated with the *StTCTP::GFP* and *GFP::GUS* constructs were incubated at 4 °C in dark for two months. Subsequently, number of shoots per tuber, length and diameter of the emerging shoot, as well as size and weight of the tubers, tubers per plant were determined with the IC Measure program (https://www.theimagingsource.com/).

4.7. Prediction of tertiary structures

4.7.1. Prediction of 3D structures of mRNA

mRNA sequences of *StTCTP*, *AtTCTP1*, *AtTCTP2*, *CmTCTP* and *StBEL5* were obtained from the Phytozome (phytozome-next.jgi.doe.gov/) and NCBI databases (https://www.ncbi.nlm.nih.gov/) (Table S8). Each sequence was uploaded in RNAFold web server (http:// rna.tbi.univie.ac.at/cgi-bin/RNAWebSuite/RNAfold.cgi) selecting the minimum free energy (MFE) and partition function algorithm to obtain the secondary structure with its Vienna format [68]. The 3D structure of the mRNAs was generated in the 3dRNA web Server (http://biophy.hust.edu.cn/3dRNA) by entering the transcript sequence and the Vienna format, choosing the option to generate 5 optimized predictions [69,70], which were analyzed in MolProbity (http://molprobity.biochem.duke.edu/) with the Nucleic Acid criteria, Geometry, Chiral handedness swaps and Tetrahedral geometry outliers to perform the comparisons [71]. In addition, EMDataResource Pseudotorsion Plot Beta Server (https://ptp.emdataresource.org/index.html) was used to evaluate the best models based on virtual torsion angles generating pseudotorsion plots for RNA that are analogous to Ramachandran plots for proteins [72]. The model with the best scores and criteria was chosen for further analysis.

4.7.2. Prediction of 3D structures of proteins

Prediction of the hypothesized 3D structure of StPTB1 and StPTB6 [57,58] was performed in the AlphaFold Colab Notebook program (AlphaFold.ipynb), which is an artificial intelligence (AI) algorithm that starts from the primary sequence of a protein to predict the 3D protein structure by

incorporating neural network architectures and training procedures based on the evolutionary, physical and geometric constraints of protein structures [73,74]. The obtained model was evaluated and refined in the DeepRefiner web server (http://watson.cse.eng.auburn.edu/DeepRefiner/index.php) that uses deep learning to generate new models [75] which were analyzed using MolProbity scores for proteins and Saves v60 (https://saves.mbi.ucla.edu/) which is a server for programs commonly used in protein structure validation [76–78] selecting the models with the best scores (ERRAT, Verify 3D, PROCHECK and Ramachandran).

4.7.3. Protein-RNA interactions by molecular docking simulation

Protein-RNA docking was performed in HDOCK (http://hdock.phys.hust.edu.cn/), based on a hybrid algorithm of template-based modeling and *ab initio* free docking [79,80]. PDB corresponding to the proteins PTB1 and PTB6 were introduced with the ligand in PDB of the *StTCTP*, *CmTCTP*, *AtTCTP1*, *AtTCTP2* and *BEL5* mRNAs, independently. The model with the highest confidence score was analyzed and visualized in UCSF Chimera and 1.16 and UCSF ChimeraX 1.5 [81,82].

4.8. Statistical analysis

Phenotype quantification was analyzed using GraphPad Prism version 8.0.0 for Windows, GraphPad Software, San Diego, California USA (https://www.graphpad.com/) with the Mann–Whitney U test with a two-tailed P value (P>0.05).

5. Conclusions

TCTP has diverse functions related to cell proliferation, regulation of programmed cell death, response to pathogens and regeneration in plants. In addition, some members of this family function in a non-cell autonomous manner, protein, mRNA or both. In the present study, through transient transformation of potato, we found evidence that the *StTCTP* transcript is transported long-distance to the apex and to roots. Furthermore, it may have a role in tuber induction and in regeneration, which in turn, suggests a role in asexual reproduction in this plant species. More work is required to determine the pathway through which *StTCTP* may regulate these processes.

Supplementary Materials: The following supporting information can be downloaded at the website of this paper posted on Preprints.org, Figure S1: *GFP* and *GAPDH* mRNA detection in agroinfiltrated and systemic leaves from potato plants transiently transformed with *GFP::GUS* construct. Figure S2: Endogenous *StTCTP* transcript levels. Figure S3: Phenotype of agroinfiltrated plants with *StTCTP::GFP* or *GFP::GUS* constructions. Figure S4: *In silico* docking analysis of TCTP transcripts and PTB1/6 proteins. Table S1: Number of tubers obtained from plants agroinfiltrated with *StTCTP::GFP* or *GFP::GUS* vectors. Table S2: MolProbity score calculation of 3D mRNA models. Table S3: mRNA Structure Validation: Pseudotorsion Plots. Table S4: MolProbity score calculation of PTB1 and PTB6 models. Table S5: Structure validation score (SAVES v6.0) of PTB1 and PTB6 refined models. Table S6: Quality of docking structures predicted in HDock. Table S7: List of oligonucleotide sequences. Table S8: Accession numbers of mRNA sequences used for 3D predictions.

Funding: This study was funded by the Biotechnology and Bioengineering Department, CINVESTAV-IPN. BX-M acknowledges doctoral fellowship (No. 636235) support by Consejo Nacional de Ciencia y Tecnología (CONACYT).

Conflicts of Interest: The authors declare no conflict of interest.

References

1. Bommer: U.-A.; Thiele, B.-J. The Translationally Controlled Tumour Protein (TCTP). *The International Journal of Biochemistry & Cell Biology* **2004**, *36*, 379–385, doi:10.1016/S1357-2725(03)00213-9.
2. Zhang, D.; Li, F.; Weidner, D.; Mnjoyan, Z.H.; Fujise, K. Physical and Functional Interaction between Myeloid Cell Leukemia 1 Protein (MCL1) and Fortilin. *Journal of Biological Chemistry* **2002**, *277*, 37430–37438, doi:10.1074/jbc.M207413200.
3. Liu, H.; Peng, H.-W.; Cheng, Y.-S.; Yuan, H.S.; Yang-Yen, H.-F. Stabilization and Enhancement of the Antiapoptotic Activity of Mcl-1 by TCTP. *Molecular and Cellular Biology* **2005**, *25*, 3117–3126, doi:10.1128/MCB.25.8.3117-3126.2005.

4. Yang, Y.; Yang, F.; Xiong, Z.; Yan, Y.; Wang, X.; Nishino, M.; Mirkovic, D.; Nguyen, J.; Wang, H.; Yang, X.-F. An N-Terminal Region of Translationally Controlled Tumor Protein Is Required for Its Antiapoptotic Activity. *Oncogene* **2005**, *24*, 4778–4788, doi:10.1038/sj.onc.1208666.
5. Rinnerthaler, M.; Jarolim, S.; Heeren, G.; Palle, E.; Perju, S.; Klinger, H.; Bogengruber, E.; Madeo, F.; Braun, R.J.; Breitenbach-Koller, L.; et al. MMI1 (YKL056c, TMA19), the Yeast Orthologue of the Translationally Controlled Tumor Protein (TCTP) Has Apoptotic Functions and Interacts with Both Microtubules and Mitochondria. *Biochimica et Biophysica Acta (BBA) - Bioenergetics* **2006**, *1757*, 631–638, doi:10.1016/j.bbabio.2006.05.022.
6. Mak, C.H.; Poon, M.W.; Lun, H.M.; Kwok, P.Y.; Ko, R.C. Heat-Inducible Translationally Controlled Tumor Protein of Trichinella Pseudospiralis: Cloning and Regulation of Gene Expression. *Parasitol Res* **2007**, *100*, 1105–1111, doi:10.1007/s00436-006-0373-y.
7. Betsch, L.; Boltz, V.; Brioudes, F.; Pontier, G.; Girard, V.; Savarin, J.; Wipperman, B.; Chambrier, P.; Tissot, N.; Benhamed, M.; et al. TCTP and CSN4 Control Cell Cycle Progression and Development by Regulating CULLIN1 Neddylation in Plants and Animals. *PLoS Genet* **2019**, *15*, e1007899, doi:10.1371/journal.pgen.1007899.
8. Li, S.; Ge, F. Current Understanding of the TCTP Interactome. In *TCTP/tpt1 - Remodeling Signaling from Stem Cell to Disease*; Telerman, A., Amson, R., Eds.; Results and Problems in Cell Differentiation; Springer International Publishing: Cham, 2017; Vol. 64, pp. 127–136 ISBN 978-3-319-67590-9.
9. Li, F.; Zhang, D.; Fujise, K. Characterization of Fortilin, a Novel Antiapoptotic Protein. *Journal of Biological Chemistry* **2001**, *276*, 47542–47549, doi:10.1074/jbc.M108954200.
10. Acunzo, J.; Baylot, V.; So, A.; Rocchi, P. TCTP as Therapeutic Target in Cancers. *Cancer Treatment Reviews* **2014**, *40*, 760–769, doi:10.1016/j.ctrv.2014.02.007.
11. Thébault, S.; Agez, M.; Chi, X.; Stojko, J.; Cura, V.; Telerman, S.B.; Maillet, L.; Gautier, F.; Billas-Massobrio, I.; Birck, C.; et al. TCTP Contains a BH3-like Domain, Which Instead of Inhibiting, Activates Bcl-XL. *Sci Rep* **2016**, *6*, 19725, doi:10.1038/srep19725.
12. Susini, L.; Besse, S.; Duflaut, D.; Lespagnol, A.; Beekman, C.; Fiucci, G.; Atkinson, A.R.; Busso, D.; Poussin, P.; Marine, J.-C.; et al. TCTP Protects from Apoptotic Cell Death by Antagonizing Bax Function. *Cell Death Differ* **2008**, *15*, 1211–1220, doi:10.1038/cdd.2008.18.
13. Jung, J.; Kim, H.Y.; Maeng, J.; Kim, M.; Shin, D.H.; Lee, K. Interaction of Translationally Controlled Tumor Protein with Apaf-1 Is Involved in the Development of Chemoresistance in HeLa Cells. *BMC Cancer* **2014**, *14*, 165, doi:10.1186/1471-2407-14-165.
14. Rho, S.B.; Lee, J.H.; Park, M.S.; Byun, H.-J.; Kang, S.; Seo, S.-S.; Kim, J.-Y.; Park, S.-Y. Anti-Apoptotic Protein TCTP Controls the Stability of the Tumor Suppressor P53. *FEBS Letters* **2011**, *585*, 29–35, doi:10.1016/j.febslet.2010.11.014.
15. Amson, R.; Pece, S.; Lespagnol, A.; Vyas, R.; Mazzarol, G.; Tosoni, D.; Colaluca, I.; Viale, G.; Rodrigues-Ferreira, S.; Wynendaele, J.; et al. Reciprocal Repression between P53 and TCTP. *Nat Med* **2012**, *18*, 91–99, doi:10.1038/nm.2546.
16. Gnanasekar, M.; Dakshinamoorthy, G.; Ramaswamy, K. Translationally Controlled Tumor Protein Is a Novel Heat Shock Protein with Chaperone-like Activity. *Biochemical and Biophysical Research Communications* **2009**, *386*, 333–337, doi:10.1016/j.bbrc.2009.06.028.
17. Lucibello, M.; Gambacurta, A.; Zonfrillo, M.; Pierimarchi, P.; Serafino, A.; Rasi, G.; Rubartelli, A.; Garaci, E. TCTP Is a Critical Survival Factor That Protects Cancer Cells from Oxidative Stress-Induced Cell-Death. *Experimental Cell Research* **2011**, *317*, 2479–2489, doi:10.1016/j.yexcr.2011.07.012.
18. Graidist, P.; Yazawa, M.; Tonganunt, M.; Nakatomi, A.; Lin, C.C.-J.; Chang, J.-Y.; Phongdara, A.; Fujise, K. Fortilin Binds Ca2+ and Blocks Ca2+-Dependent Apoptosis *in Vivo*. *Biochemical Journal* **2007**, *408*, 181–191, doi:10.1042/BJ20070679.
19. Gachet, Y.; Tournier, S.; Lee, M.; Lazaris-Karatzas, A.; Poulton, T.; Bommer, U.A. The Growth-Related, Translationally Controlled Protein P23 Has Properties of a Tubulin Binding Protein and Associates Transiently with Microtubules during the Cell Cycle. *Journal of Cell Science* **1999**, *112*, 1257–1271, doi:10.1242/jcs.112.8.1257.
20. Tani, T.; Shimada, H.; Kato, Y.; Tsunoda, Y. Bovine Oocytes with the Potential to Reprogram Somatic Cell Nuclei Have a Unique 23-KDa Protein, Phosphorylated Transcriptionally Controlled Tumor Protein (TCTP). *Cloning and Stem Cells* **2007**, *9*, 267–280, doi:10.1089/clo.2006.0072.

21. Jeon, H.-J.; You, S.Y.; Park, Y.S.; Chang, J.W.; Kim, J.-S.; Oh, J.S. TCTP Regulates Spindle Microtubule Dynamics by Stabilizing Polar Microtubules during Mouse Oocyte Meiosis. *Biochimica et Biophysica Acta (BBA) - Molecular Cell Research* **2016**, *1863*, 630–637, doi:10.1016/j.bbamcr.2016.01.012.
22. Chen, S.H.; Wu, P.-S.; Chou, C.-H.; Yan, Y.-T.; Liu, H.; Weng, S.-Y.; Yang-Yen, H.-F. A Knockout Mouse Approach Reveals That TCTP Functions as an Essential Factor for Cell Proliferation and Survival in a Tissue- or Cell Type–Specific Manner. *MBoC* **2007**, *18*, 2525–2532, doi:10.1091/mbc.e07-02-0188.
23. Koide, Y.; Kiyota, T.; Tonganunt, M.; Pinkaew, D.; Liu, Z.; Kato, Y.; Hutadilok-Towatana, N.; Phongdara, A.; Fujise, K. Embryonic Lethality of Fortilin-Null Mutant Mice by BMP-Pathway Overactivation. *Biochimica et Biophysica Acta (BBA) - General Subjects* **2009**, *1790*, 326–338, doi:10.1016/j.bbagen.2009.01.012.
24. Hsu, Y.-C.; Chern, J.J.; Cai, Y.; Liu, M.; Choi, K.-W. Drosophila TCTP Is Essential for Growth and Proliferation through Regulation of DRheb GTPase. *Nature* **2007**, *445*, 785–788, doi:10.1038/nature05528.
25. Hong, S.-T.; Choi, K.-W. TCTP Directly Regulates ATM Activity to Control Genome Stability and Organ Development in Drosophila Melanogaster. *Nat Commun* **2013**, *4*, 2986, doi:10.1038/ncomms3986.
26. Brioudes, F.; Thierry, A.-M.; Chambrier, P.; Mollereau, B.; Bendahmane, M. Translationally Controlled Tumor Protein Is a Conserved Mitotic Growth Integrator in Animals and Plants. *Proc. Natl. Acad. Sci. U.S.A.* **2010**, *107*, 16384–16389, doi:10.1073/pnas.1007926107.
27. Ma, X.M.; Blenis, J. Molecular Mechanisms of MTOR-Mediated Translational Control. *Nat Rev Mol Cell Biol* **2009**, *10*, 307–318, doi:10.1038/nrm2672.
28. Bommer, U.-A.; Iadevaia, V.; Chen, J.; Knoch, B.; Engel, M.; Proud, C.G. Growth-Factor Dependent Expression of the Translationally Controlled Tumour Protein TCTP Is Regulated through the PI3-K/Akt/MTORC1 Signalling Pathway. *Cellular Signalling* **2015**, *27*, 1557–1568, doi:10.1016/j.cellsig.2015.04.011.
29. Kim, Y.-M.; Han, Y.-J.; Hwang, O.-J.; Lee, S.-S.; Shin, A.-Y.; Kim, S.Y.; Kim, J.-I. Overexpression of Arabidopsis Translationally Controlled Tumor Protein Gene AtTCTP Enhances Drought Tolerance with Rapid ABA-Induced Stomatal Closure. *Mol Cells* **2012**, *33*, 617–626, doi:10.1007/s10059-012-0080-8.
30. De Carvalho, M.; Acencio, M.L.; Laitz, A.V.N.; De Araújo, L.M.; De Lara Campos Arcuri, M.; Do Nascimento, L.C.; Maia, I.G. Impacts of the Overexpression of a Tomato Translationally Controlled Tumor Protein (TCTP) in Tobacco Revealed by Phenotypic and Transcriptomic Analysis. *Plant Cell Rep* **2017**, *36*, 887–900, doi:10.1007/s00299-017-2117-0.
31. Berkowitz, O.; Jost, R.; Pollmann, S.; Masle, J. Characterization of TCTP, the Translationally Controlled Tumor Protein, from *Arabidopsis Thaliana*. *The Plant Cell* **2009**, *20*, 3430–3447, doi:10.1105/tpc.108.061010.
32. Liao, F.; Wang, L.; Yang, L.-B.; Peng, X.; Sun, M. NtGNL1 Plays an Essential Role in Pollen Tube Tip Growth and Orientation Likely via Regulation of Post-Golgi Trafficking. *PLoS ONE* **2010**, *5*, e13401, doi:10.1371/journal.pone.0013401.
33. Zou, X.; Li, L.; Liao, F.; Chen, W. ITRAQ-Based Quantitative Proteomic Analysis Reveals NtGNL1-Dependent Regulatory Network Underlying Endosome Trafficking for Pollen Tube Polar Growth. *Plant Physiology and Biochemistry* **2021**, *161*, 200–209, doi:10.1016/j.plaphy.2021.02.010.
34. Corbesier, L.; Vincent, C.; Jang, S.; Fornara, F.; Fan, Q.; Searle, I.; Giakountis, A.; Farrona, S.; Gissot, L.; Turnbull, C.; et al. FT Protein Movement Contributes to Long-Distance Signaling in Floral Induction of *Arabidopsis*. *Science* **2007**, *316*, 1030–1033, doi:10.1126/science.1141752.
35. Pant, B.D.; Buhtz, A.; Kehr, J.; Scheible, W.-R. MicroRNA399 Is a Long-Distance Signal for the Regulation of Plant Phosphate Homeostasis. *Plant J* **2008**, *53*, 731–738, doi:10.1111/j.1365-313X.2007.03363.x.
36. Zhang, Z.; Zheng, Y.; Ham, B.-K.; Chen, J.; Yoshida, A.; Kochian, L.V.; Fei, Z.; Lucas, W.J. Vascular-Mediated Signalling Involved in Early Phosphate Stress Response in Plants. *Nature Plants* **2016**, *2*, 16033, doi:10.1038/nplants.2016.33.
37. Yoo, B.-C.; Kragler, F.; Varkonyi-Gasic, E.; Haywood, V.; Archer-Evans, S.; Lee, Y.M.; Lough, T.J.; Lucas, W.J. A Systemic Small RNA Signaling System in Plants. *Plant Cell* **2004**, *16*, 1979–2000, doi:10.1105/tpc.104.023614.
38. Champigny, M.J.; Isaacs, M.; Carella, P.; Faubert, J.; Fobert, P.R.; Cameron, R.K. Long Distance Movement of DIR1 and Investigation of the Role of DIR1-like during Systemic Acquired Resistance in Arabidopsis. *Front. Plant Sci.* **2013**, *4*, doi:10.3389/fpls.2013.00230.
39. Martin, A.; Adam, H.; Díaz-Mendoza, M.; Żurczak, M.; González-Schain, N.D.; Suárez-López, P. Graft-Transmissible Induction of Potato Tuberization by the MicroRNA *MiR172*. *Development* **2009**, *136*, 2873–2881, doi:10.1242/dev.031658.

40. Navarro, C.; Abelenda, J.A.; Cruz-Oró, E.; Cuéllar, C.A.; Tamaki, S.; Silva, J.; Shimamoto, K.; Prat, S. Control of Flowering and Storage Organ Formation in Potato by FLOWERING LOCUS T. *Nature* **2011**, *478*, 119–122, doi:10.1038/nature10431.
41. Peres, L.E.P.; Carvalho, R.F.; Zsögön, A.; Bermúdez-Zambrano, O.D.; Robles, W.G.R.; Tavares, S. Grafting of Tomato Mutants onto Potato Rootstocks: An Approach to Study Leaf-Derived Signaling on Tuberization. *Plant Science* **2005**, *169*, 680–688, doi:10.1016/j.plantsci.2005.05.017.
42. Rosin, F.M.; Hart, J.K.; Horner, H.T.; Davies, P.J.; Hannapel, D.J. Overexpression of a *Knotted* -Like Homeobox Gene of Potato Alters Vegetative Development by Decreasing Gibberellin Accumulation. *Plant Physiology* **2003**, *132*, 106–117, doi:10.1104/pp.102.015560.
43. Yu, Y.; Lashbrook, C.C.; Hannapel, D.J. Tissue Integrity and RNA Quality of Laser Microdissected Phloem of Potato. *Planta* **2007**, *226*, 797–803, doi:10.1007/s00425-007-0509-z.
44. Campbell, B.A.; Hallengren, J.; Hannapel, D.J. Accumulation of BEL1-like Transcripts in Solanaceous Species. *Planta* **2008**, *228*, 897–906, doi:10.1007/s00425-008-0780-7.
45. Mahajan, A.; Bhogale, S.; Kang, I.H.; Hannapel, D.J.; Banerjee, A.K. The MRNA of a Knotted1-like Transcription Factor of Potato Is Phloem Mobile. *Plant Mol Biol* **2012**, *79*, 595–608, doi:10.1007/s11103-012-9931-0.
46. Banerjee, A.K.; Chatterjee, M.; Yu, Y.; Suh, S.-G.; Miller, W.A.; Hannapel, D.J. Dynamics of a Mobile RNA of Potato Involved in a Long-Distance Signaling Pathway. *The Plant Cell* **2007**, *18*, 3443–3457, doi:10.1105/tpc.106.042473.
47. Hinojosa-Moya, J.J.; Xoconostle-Cázares, B.; Toscano-Morales, R.; Ramírez-Ortega, F.; Luis Cabrera-Ponce, J.; Ruiz-Medrano, R. Characterization of the Pumpkin Translationally-Controlled Tumor Protein *CmTCTP*. *Plant Signaling & Behavior* **2013**, *8*, e26477, doi:10.4161/psb.26477.
48. Toscano-Morales, R.; Xoconostle-Cázares, B.; Martínez-Navarro, A.C.; Ruiz-Medrano, R. Long Distance Movement of an Arabidopsis Translationally Controlled Tumor Protein (AtTCTP2) MRNA and Protein in Tobacco. *Front. Plant Sci.* **2014**, *5*, doi:10.3389/fpls.2014.00705.
49. Toscano-Morales, R.; Xoconostle-Cázares, B.; Cabrera-Ponce, J.L.; Hinojosa-Moya, J.; Ruiz-Salas, J.L.; Galván-Gordillo, S.V.; Guevara-González, R.G.; Ruiz-Medrano, R. AtTCTP2, an Arabidopsis Thaliana Homolog of Translationally Controlled Tumor Protein, Enhances in Vitro Plant Regeneration. *Front. Plant Sci.* **2015**, *6*, doi:10.3389/fpls.2015.00468.
50. Thieme, C.J.; Rojas-Triana, M.; Stecyk, E.; Schudoma, C.; Zhang, W.; Yang, L.; Miñambres, M.; Walther, D.; Schulze, W.X.; Paz-Ares, J.; et al. Endogenous Arabidopsis Messenger RNAs Transported to Distant Tissues. *Nature Plants* **2015**, *1*, 15025, doi:10.1038/nplants.2015.25.
51. Doering-Saad, C.; Newbury, H.; Couldridge, C.; Bale, J.; Pritchard, J. A Phloem-Enriched CDNA Library from Ricinus: Insights into Phloem Function. *Journal of Experimental Botany* **2006**, *57*, 3183–3193, doi:10.1093/jxb/erl082.
52. Giavalisco, P.; Kapitza, K.; Kolasa, A.; Buhtz, A.; Kehr, J. Towards the Proteome OfBrassica Napus Phloem Sap. *Proteomics* **2006**, *6*, 896–909, doi:10.1002/pmic.200500155.
53. Rodriguez-Medina, C.; Atkins, C.A.; Mann, A.J.; Jordan, M.E.; Smith, P.M. Macromolecular Composition of Phloem Exudate from White Lupin (Lupinus AlbusL.). *BMC Plant Biol* **2011**, *11*, 36, doi:10.1186/1471-2229-11-36.
54. Toscano-Morales, R.; Xoconostle-Cázares, B.; Martínez-Navarro, A.C.; Ruiz-Medrano, R. *AtTCTP2* MRNA and Protein Movement Correlates with Formation of Adventitious Roots in Tobacco. *Plant Signaling & Behavior* **2016**, *11*, e1071003, doi:10.1080/15592324.2015.1071003.
55. Gutiérrez-Galeano, D.F.; Toscano-Morales, R.; Calderón-Pérez, B.; Xoconostle-Cázares, B.; Ruiz-Medrano, R. Structural Divergence of Plant TCTPs. *Front. Plant Sci.* **2014**, *5*, doi:10.3389/fpls.2014.00361.
56. Weeda, S.M.; Mohan Kumar, G.N.; Richard Knowles, N. Developmentally Linked Changes in Proteases and Protease Inhibitors Suggest a Role for Potato Multicystatin in Regulating Protein Content of Potato Tubers. *Planta* **2009**, *230*, 73–84, doi:10.1007/s00425-009-0928-0.
57. Cho, S.K.; Sharma, P.; Butler, N.M.; Kang, I.-H.; Shah, S.; Rao, A.G.; Hannapel, D.J. Polypyrimidine Tract-Binding Proteins of Potato Mediate Tuberization through an Interaction with *StBEL5* RNA. *EXBOTJ* **2015**, *66*, 6835–6847, doi:10.1093/jxb/erv389.
58. Kondhare, K.R.; Kumar, A.; Hannapel, D.J.; Banerjee, A.K. Conservation of Polypyrimidine Tract Binding Proteins and Their Putative Target RNAs in Several Storage Root Crops. *BMC Genomics* **2018**, *19*, 124, doi:10.1186/s12864-018-4502-7.
59. Reuveni, M. Sex and Regeneration. *Biology* **2021**, *10*, 937, doi:10.3390/biology10090937.

60. Yang, L.; Perrera, V.; Saplaoura, E.; Apelt, F.; Bahin, M.; Kramdi, A.; Olas, J.; Mueller-Roeber, B.; Sokolowska, E.; Zhang, W.; et al. M5C Methylation Guides Systemic Transport of Messenger RNA over Graft Junctions in Plants. *Current Biology* **2019**, *29*, 2465-2476.e5, doi:10.1016/j.cub.2019.06.042.
61. Naing, A.H.; Kim, C.K. Abiotic Stress-induced Anthocyanins in Plants: Their Role in Tolerance to Abiotic Stresses. *Physiologia Plantarum* **2021**, *172*, 1711–1723, doi:10.1111/ppl.13373.
62. Kumlay, A.M.; Ercisli, S. Callus Induction, Shoot Proliferation and Root Regeneration of Potato (*Solanum Tuberosum* L.) Stem Node and Leaf Explants under Long-Day Conditions. *Biotechnology & Biotechnological Equipment* **2015**, *29*, 1075–1084, doi:10.1080/13102818.2015.1077685.
63. Logemann, J.; Schell, J.; Willmitzer, L. Improved Method for the Isolation of RNA from Plant Tissues. *Analytical Biochemistry* **1987**, *163*, 16–20, doi:10.1016/0003-2697(87)90086-8.
64. Nuñez-Muñoz, L.; Vargas-Hernández, B.; Hinojosa-Moya, J.; Ruiz-Medrano, R.; Xoconostle-Cázares, B. Plant Drought Tolerance Provided through Genome Editing of the Trehalase Gene. *Plant Signaling & Behavior* **2021**, *16*, 1877005, doi:10.1080/15592324.2021.1877005.
65. Mba'u, Y.J.; Iriawati; Faizal, A. Transient Transformation of Potato Plant (Solanum Tuberosum L.) Granola Cultivar Using Syringe Agroinfiltration. *Agrivita.J.Agr.Sci* **2018**, *40*, doi:10.17503/agrivita.v40i2.1467.
66. Ruiz-Salas, J.L.; Ruiz-Medrano, R.; Montes-Horcasitas, M.D.C.; Agreda-Laguna, K.A.; Hinojosa-Moya, J.; Xoconostle-Cázares, B. Vascular Expression of Trehalose Phosphate Synthase1 (TPS1) Induces Flowering in Arabidopsis. *Plant Omics* **2016**, *9*, 344–351, doi:10.21475/poj.09.05.16.pne188.
67. Livak, K.J.; Schmittgen, T.D. Analysis of Relative Gene Expression Data Using Real-Time Quantitative PCR and the 2−ΔΔCT Method. *Methods* **2001**, *25*, 402–408, doi:10.1006/meth.2001.1262.
68. Hofacker, I.L. Vienna RNA Secondary Structure Server. *Nucleic Acids Research* **2003**, *31*, 3429–3431, doi:10.1093/nar/gkg599.
69. Zhang, Y.; Xiong, Y.; Xiao, Y. 3dDNA: A Computational Method of Building DNA 3D Structures. *Molecules* **2022**, *27*, 5936, doi:10.3390/molecules27185936.
70. Zhang, Y.; Wang, J.; Xiao, Y. 3dRNA: 3D Structure Prediction from Linear to Circular RNAs. *Journal of Molecular Biology* **2022**, *434*, 167452, doi:10.1016/j.jmb.2022.167452.
71. Williams, C.J.; Headd, J.J.; Moriarty, N.W.; Prisant, M.G.; Videau, L.L.; Deis, L.N.; Verma, V.; Keedy, D.A.; Hintze, B.J.; Chen, V.B.; et al. MolProbity: More and Better Reference Data for Improved All-Atom Structure Validation: PROTEIN SCIENCE.ORG. *Protein Science* **2018**, *27*, 293–315, doi:10.1002/pro.3330.
72. Wadley, L.M.; Keating, K.S.; Duarte, C.M.; Pyle, A.M. Evaluating and Learning from RNA Pseudotorsional Space: Quantitative Validation of a Reduced Representation for RNA Structure. *Journal of Molecular Biology* **2007**, *372*, 942–957, doi:10.1016/j.jmb.2007.06.058.
73. Jumper, J.; Evans, R.; Pritzel, A.; Green, T.; Figurnov, M.; Ronneberger, O.; Tunyasuvunakool, K.; Bates, R.; Žídek, A.; Potapenko, A.; et al. Highly Accurate Protein Structure Prediction with AlphaFold. *Nature* **2021**, *596*, 583–589, doi:10.1038/s41586-021-03819-2.
74. Jumper, J.; Hassabis, D. Protein Structure Predictions to Atomic Accuracy with AlphaFold. *Nat Methods* **2022**, *19*, 11–12, doi:10.1038/s41592-021-01362-6.
75. Shuvo, M.H.; Gulfam, M.; Bhattacharya, D. DeepRefiner: High-Accuracy Protein Structure Refinement by Deep Network Calibration. *Nucleic Acids Research* **2021**, *49*, W147–W152, doi:10.1093/nar/gkab361.
76. Colovos, C.; Yeates, T.O. Verification of Protein Structures: Patterns of Nonbonded Atomic Interactions. *Protein Sci.* **1993**, *2*, 1511–1519, doi:10.1002/pro.5560020916.
77. Laskowski, R.A.; MacArthur, M.W.; Moss, D.S.; Thornton, J.M. PROCHECK: A Program to Check the Stereochemical Quality of Protein Structures. *J Appl Crystallogr* **1993**, *26*, 283–291, doi:10.1107/S0021889892009944.
78. Lüthy, R.; Bowie, J.U.; Eisenberg, D. Assessment of Protein Models with Three-Dimensional Profiles. *Nature* **1992**, *356*, 83–85, doi:10.1038/356083a0.
79. Yan, Y.; Zhang, D.; Zhou, P.; Li, B.; Huang, S.-Y. HDOCK: A Web Server for Protein–Protein and Protein–DNA/RNA Docking Based on a Hybrid Strategy. *Nucleic Acids Research* **2017**, *45*, W365–W373, doi:10.1093/nar/gkx407.
80. Yan, Y.; Tao, H.; He, J.; Huang, S.-Y. The HDOCK Server for Integrated Protein–Protein Docking. *Nat Protoc* **2020**, *15*, 1829–1852, doi:10.1038/s41596-020-0312-x.
81. Pettersen, E.F.; Goddard, T.D.; Huang, C.C.; Couch, G.S.; Greenblatt, D.M.; Meng, E.C.; Ferrin, T.E. UCSF Chimera?A Visualization System for Exploratory Research and Analysis. *J. Comput. Chem.* **2004**, *25*, 1605–1612, doi:10.1002/jcc.20084.

 doi:10.20944/preprints202306.1347.v1

82. Pettersen, E.F.; Goddard, T.D.; Huang, C.C.; Meng, E.C.; Couch, G.S.; Croll, T.I.; Morris, J.H.; Ferrin, T.E. UCSF ChimeraX : Structure Visualization for Researchers, Educators, and Developers. *Protein Science* **2021**, *30*, 70–82, doi:10.1002/pro.3943.